Eur. Phys. J. D **20**, 573–582 (2002)
DOI: 10.1140/epjd/e2002-00169-0

THE EUROPEAN PHYSICAL JOURNAL D

Analytical laser induced liquid beam desorption mass spectrometry of protonated amino acids and their non-covalently bound aggregates

A. Charvat[1], E. Lugovoj[1], M. Faubel[2], and B. Abel[1,a]

[1] MPI für Biophysikalische Chemie, Am Faßberg 11, 37077 Göttingen, Germany
[2] MPI für Strömungsforschung, Bunsenstraße 10, 37073 Göttingen, Germany

Received 28 June 2002
Published online 13 September 2002

Abstract. We have used analytical laser induced liquid beam desorption in combination with high resolution mass spectrometry ($m/\Delta m \geq 1\,000$) for the study of protonated amino acids (ornithine, citrulline, lysine, arginine) and their non-covalently bound complexes in the gas phase desorbed from water solutions. We report studies in which the desorption mechanism has been investigated. The results imply that biomolecule desorption at our conditions is a single step process involving laser heating of the solvent above its supercritical temperature, a rapid expansion, ion recombination and finally isolation and desorption of only a small fraction of preformed ions and charged aggregates. In addition, we report an investigation of the aqueous solution concentration and pH-dependence of the laser induced desorption of protonated species (monomers and dimers). The experimental findings suggest that the desorption process depends critically upon the proton affinity of the molecules, the concentration of other ions, and of the pH value of the solution. Therefore the ion concentrations measured in the gas phase very likely reflect solution properties (equilibrium concentrations). Arginine self-assembles large non-covalent singly protonated multimers ($n = 1...8$) when sampled by IR laser induced water beam desorption mass spectrometry. The structures of these aggregates may resemble those of the solid state and may be preformed in solution prior to desorption. A desorption of mixtures of amino acids in water solution enabled us to study (mixed) protonated dimers, one of the various applications of the present technique. Reasons for preferred dimerization – leading to simple cases of molecular recognition – as well as less preferred binding is discussed in terms of the number of specific H-bonds that can be established in the clusters.

PACS. 82.80.Rt Time of flight mass spectrometry – 87.15.-v Biomolecules: structure and physical properties – 87.15.Nn Properties of solutions; aggregation and crystallization of macromolecules

1 Introduction

The function of a biomolecule usually depends on its specific, non-covalent interactions with another molecule. For example, proteins interact with other proteins, peptides, small molecules, metal ions, lipids, polysaccarides, nucleic acids and oligonucleotides and these interactions drive critically important biological processes. Several well established spectroscopic techniques are used to study biomolecular interactions including circular dichroism, fluorescence, infrared and ultraviolet spectroscopy, nuclear magnetic resonance, and X-ray crystallography [1]. In the past mass spectrometry has been limited to the study of small stable molecules, however, with the emergence of electrospray ionization (ESI) [1,2] or matrix assisted laser induced desorption and ionization (MALDI) [3] large biomolecules as well as non-covalent biomolecular complexes could be studied. One technique that is emerging as a new and exciting method to study biomolecular non-covalent interactions and complexation is what we call *analytical laser induced liquid beam desorption mass spectrometry*, recently introduced by Brutschy and coworkers and termed LILBID (laser induced liquid beam ionization/desorption) [4–8]. The experimental approach enables a gentle and soft desorption of neutrals, protonated molecular species, as well as their non-covalently bound complexes with an infrared laser pulse tuned to the OH-stretch vibration of liquid water. In the case of protonated molecules or singly charged non-covalently bound complexes post-desorption ionization with a second laser [9–11] is not necessary for their sensitive detection *via* high resolution mass spectrometry. This is a significant advantage for analytic applications because it avoids fragmentation.

Amino acids are building blocks of larger biopolymers such as proteins and peptides but at the same time they are nice model systems for applications of advanced mass

[a] e-mail: babel@gwdg.de

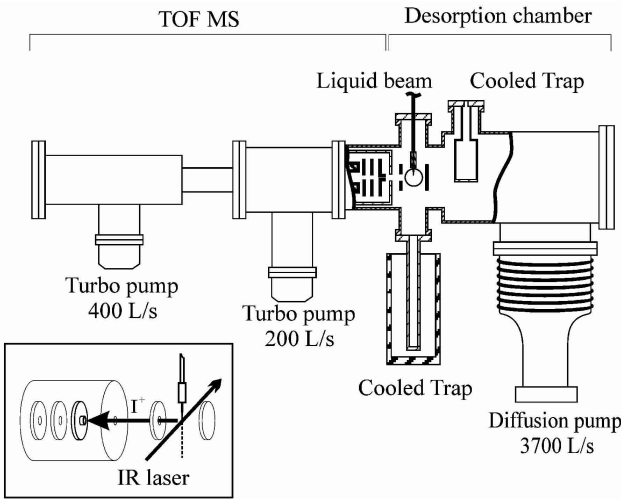

Fig. 1. Schematic experimental setup. Time-of-flight spectrometer, desorption chamber with pumps, and the high pressure nozzle setup. The inset shows the ion optics for the initial collection and for focusing of the desorbed ions, and the drift region.

spectrometric techniques. In aqueous solution or in crystalline media, they adopt charge-separated, zwitterionic structures but it is generally agreed that they all exist as neutral molecules when isolated in the gas phase or in rare gas matrixes, as do their residues in peptide chains [12]. Experimental work employing IR-spectroscopy and mass spectrometry as well as theoretical investigations provide a wealth of information about the conformation of amino acids, their zwitterionic structure and their energetics in the gas and in the condensed phase [13–18].

We have recently employed analytical laser induced liquid beam desorption in combination with high resolution mass spectrometry [19] for a detailed study of the desorption mechanism, molecular recognition and aggregation of amino acids (histidine, citrulline, ornithine, arginine, lysine).

2 Experimental

Figure 1 shows a schematic diagram of the experimental apparatus used in the present study. It consists of a liquid beam [20–22], an IR laser system, and a reflectron time-of-flight mass spectrometer (TOF-MS) (Kaesdorf) [19]. A continuous liquid flow (liquid beam) was introduced downward into a vacuum chamber through a quartz nozzle with an inner diameter of 17 μm, forming a water beam of about 11 μm thickness. The temperature controlled liquid water was pumped through a sequence of filters and finally through the nozzle at 10 bar with a HPLC pump (Gynkotek, Model 300C), designed for liquid chromatography. The flow rate was kept constant at 0.4 ml/min throughout the experiment. A solution of the amino acids in pure water with concentrations between 0.1 and 10^{-6} mol/liter was employed in the present studies. The liquid beam was trapped in a cold trap about 20 cm downstream from the nozzle. The chamber was evacuated down to 5×10^{-5} mbar by a 3 700 l/s diffusion pump and a cryo-trap. Traveling a distance of 1–2 mm from the quartz nozzle exit, the liquid beam was crossed with a IR laser beam ($\lambda = 2.735$ μm) in the first ion optics. The IR wavelength is tuned into resonance with the fundamental of the OH stretch vibration of bulk water, such that only the solvent molecules are excited in the water beam. The IR laser beam was generated from the fundamental of a Nd:YAG laser (Continuum, NY81C-20) and a dye laser pulse at 766 nm, that was pumped by the same Nd:YAG laser, *via* difference frequency generation in a $LiNbO_3$ crystal (INRAD^{TM}, Autotracker III). The output energy was between 0.5 and 1 mJ/pulse. The infrared wavelength was separated from the fundamentals with a germanium plate. The IR laser pulse was expanded and tightly focused onto the water beam with a three lens system. The threshold intensity for desorption at the water beam was estimated to be around 10^8 W/cm^2. Neutral species, bare solute molecules, clusters composed of solute and solvent molecules, as well as their protonated counterparts are desorbed from the beam. Without an additional post-desorption laser pulse only the protonated molecules and aggregates can be detected. In the direction perpendicular to both the laser and the water beam the produced ions are accelerated and collimated in an ion optics with a continuous electric field (typically 100 V/cm) into two differentially pumped vacuum chambers containing the ion optics of the TOF spectrometer [19]. The field free drift region before entering the TOF ion optics was 35 mm. The three electrode optics of the TOF reflectron mass spectrometer was set to fulfill the Wiley-McLaren criterion and pulsed (up to 10 kV) with two commercial high voltage switches (Behlke). The ion optics also worked as a gate for the selection of different masses (monomers, dimers) from the desorption process. The ions were then steered and focused by a set of vertical and horizontal deflectors and an einzel lens. After traveling about 600 mm in the field free region, the ions were reversed by the reflectron tilted about 5 degrees off the beam axis (1 050 mm total field free region). After passing the ion mirror and the second drift region of the spectrometer the ions were post-accelerated in front of the multichannel plate detector to 10 kV. The signals were amplified and recorded with a 200 MHz digital oscilloscope (Tektronix) and a 200 MHz digitizer card (Acqiris^{TM}) in a computer operated under LABVIEW^{TM}. A Stanford Research Systems DG535 digital delay generator varied the timing of (the IR laser and) the ion optics. The mass resolution $m/\Delta m$ of the experiment was usually well above 1 000 in the mass range between 100 and 500 amu. All amino acids (L-form), their HCl adducts, and water (UVASOL^{TM}) were purchased from Merck and used without further purification.

3 Results and discussion

3.1 Protonated dimers and multimers of amino acids

In the present investigation amino acids serve as model systems to demonstrate the ability of the present approach

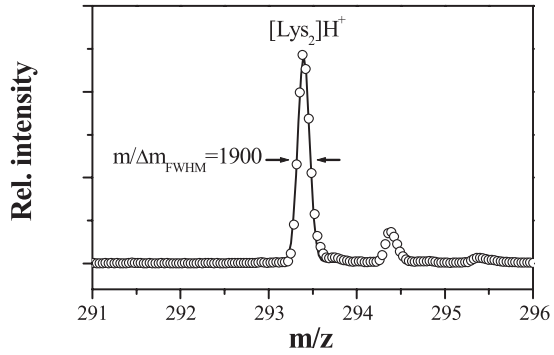

Fig. 2. Time-of-flight spectrum of protonated lysine dimers. The satellite peaks at higher masses correspond to ^{13}C isotopes. The solid line is a fit for the determination of the mass resolution of the system ($m/\Delta m = 1\,900$ in this case).

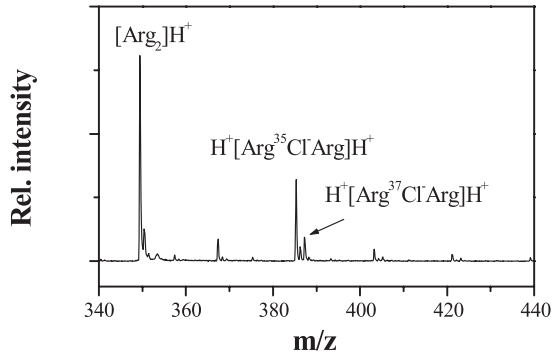

Fig. 3. Time-of-flight spectrum stable adducts of protonated arginine dimers with Cl^- anions. Desorption from a 10^{-2} molar solution of arginine hydrochloride in water.

to investigate non-covalently bound complexes, *i.e.*, protonated amino acid multimers. For moderate concentrations (10^{-1}–10^{-3} molar) of the amino acids or their HCl adducts (salts) in water, significant amounts of protonated multimers, particularly dimers, were observed when sampled with analytical water beam desorption mass spectrometry. Figure 2 displays the time-of-flight spectrum of protonated lysine dimers. The solid line is a fit for the determination of the mass resolution of the system. The satellite peaks on the right hand side correspond to ^{13}C-isotopes of the dimers which are easily resolvable. It has also been found that particularly stable and abundant adducts with anions present in the solution can be detected easily. Figure 3 displays a spectrum of the $((HArg)_2\ Cl)^+$ aggregate that appears to be quite stable. It is formed by two protonated arginines and a Cl^- ion. This result again underscores one important feature of the technique, namely the nearly fragmentation free desorption of biomolecules and their non-covalently bound complexes and their detection by adduct formation (protons, anions, but also cations).

The crucial question that now arises is whether the complexes, *i.e.*, multimers, are preformed in solution and subsequently desorbed, or if they are formed in the gas phase in the expansion region of the desorption process. In general, this question is not easy to answer for the present technique nor for any of the competitive techniques in the field like MALDI or ESI. One more or less convincing approach would be if it is possible to create defined concentrations of species in solution that are imaged in the intensity patterns of mass spectra present in gas phase measurements. A measurement of protonation equilibria as a function of the pH value and/or temperature would in principle provide conclusive evidence for the desorption of preformed ions. Also an imaging of other defined solution equilibria like dimerization or complexation as a function of any solution parameter would be suitable. In a series of experiments Brutschy and co-workers have shown that the desorption of non-covalently bound species is correlated with protonation equilibria in solution and that complexation in solution is imaged in the gas phase mass spectra [4,23]. In particular, the temperature and pH dependence of protonation equilibria of amides in solution appears to be imaged in the corresponding gas phase mass peaks [23]. From this work is appears to be very likely that analytical laser induced liquid beam desorption can in fact display solution properties like equilibrium concentrations or preformed non-covalently bound complexes and aggregates in solution, and project the quantities on intensities of mass peaks in the gas phase.

For the present case of amino acids and their multimers in aqueous solution it is known that protonation equilibria depend upon the proton affinity of the amino acids [24]. For our amino acids under investigation the equilibrium concentrations of singly and doubly protonated amino acids, zwitterionic species, and anionic species can be calculated from known pK_s-data or proton affinity data [24]. In the positive ion detection mode of our spectrometer we are only able to monitor cations or positively charged aggregates. Analytical laser induced liquid beam desorption is known to produce mostly singly charged species as opposed to the ESI-technique [1,2,4–6]. Therefore, the detectable signal of singly protonated amino acids and multimers in the experiment should depend upon the H_3O^+ (pH value) as well as the amino acid concentration of the aqueous solution in a defined fashion. In addition, the yield of desorption of preformed ions in solution should depend upon the presence of other ionic species in the solution, because the desorption yield is affected by ion pair recombination which can be expected to be a function of the ionic strength of the solution.

A series of systematic experiments along these lines is shown in Figure 4. In these experiments the concentration (top to bottom) and pH dependence (right to left) of the desorption signals of singly protonated monomers and dimers of citrulline is shown. In order to avoid confusion, we note that the plots in Figure 4 display gas phase mass spectra. The pH value and the concentrations of the corresponding solutions are given as labels. In the following the gas phase mass spectra are discussed as a function of the changed solution parameters without, however, assuming a correlation between solution parameters and mass peaks in the gas phase *a priori*. For pH = 5, the proton concentration of the solution is limited and it is reasonable to assume that the same holds for the concentration of

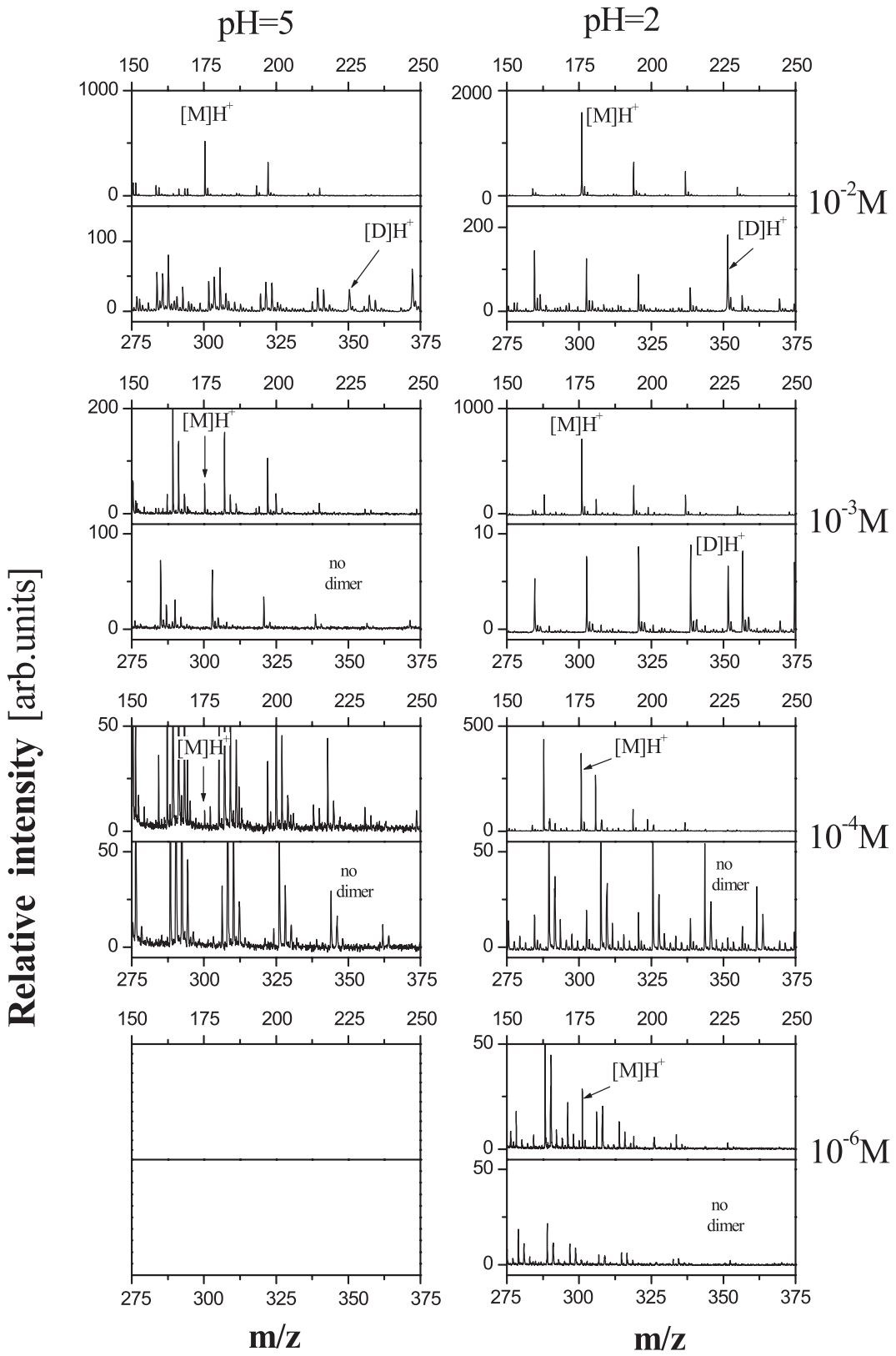

Fig. 4. Concentration dependence (vertical series) and pH-dependence (left and right) of the desorption of citrulline in water (between 10^{-2} and 10^{-6} mol/l and for pH = 2 (H_2SO_4) and pH = 5). Shown are signals for optimum gate times for the monomer and the dimer, respectively. Note, M and D refer to the monomer and the dimer respectively. In addition, we note that the majority of the mass peaks in the plots result from pure protonated water clusters ($H^+(H_2O)_n$) and some of them from protonated amino acid (dimer) water clusters. For more details see the text.

protonated citrulline. This manifests itself in a somewhat reduced gas phase ion signal as opposed to the pH = 2 case, which is discussed below. In the left column of Figure 4 the dependence of the mass spectra of desorbed protonated monomers and dimers in the gas phase as a function of solution concentration is displayed. It is obvious that mass peaks of the monomer roughly scale with the amino acid concentration of the solution. Relative peak intensities of protonated monomers and dimers reflect the dimerization equilibrium of amino acids in aqueous solution. It should be noted, that most of the mass peaks in Figure 4 result from pure protonated water clusters ($H^+(H_2O)_n$) and some of them from protonated amino acid (dimer) water clusters. For the latter case the number of monomer (dimer) sample ions in the gas phase is proportional to the sum over all formed monomer (dimer) water clusters, which has to be taken into account when determining monomer to dimer concentration ratios. It is obvious that the peaks of the protonated dimer (in the gas phase) disappear at solution concentrations below 1×10^{-2} mol/l. This is in agreement with a $[M]^2$ dependence of preformed protonated dimers in solution as predicted form the equilibrium expression.

Although equilibrium constants for dimerization and the formation of multimers of amino acids have been measured by voltametry [25], unfortunately, for the present set of amino acids there exist no data to compare with. It is interesting to note that for the range of concentrations investigated in this study the concentration of desorbed (protonated) dimers are quite significant. This feature can be rationalized if one considers the ability of amino acids to form strong double salt bridge bonds. For pH > 7 ion signals other than protonated water clusters were difficult to detect.

In contrast to the previous column of experiments, for pH = 2, the monomer and the dimer intensities in the mass spectra (in the gas phase) are much higher and they can be detected with a good signal-to-noise ratio even down to 1×10^{-6} mol/l. We attribute this to the much higher cation concentration in solution that can be desorbed in the experiment, which is a direct consequence of the higher pH. As in the previous case (pH = 5) we expected a simple scaling of the ion signals with amino acid concentration. Instead, we found a much more complicated dependence of the mass peaks of protonated monomers and dimers upon the concentration of the solution. The difference in the ion signal for pH = 2 and pH = 5 is striking. Even more striking is that the ratio of the monomer peaks at pH = 2 and pH = 5 is not constant, instead it is decreasing for increasing concentration of the solution. The mass peaks for protonated dimers in the gas phase follow the expected trend, *i.e.*, they appear to correlate with predicted preformed protonated dimers in solution and display the expected concentration dependence. Interestingly, the experimental findings imply a pronounced saturation behavior (as far as desorption of protonated species is concerned) when increasing the concentration of the solution between 10^{-6} M to 10^{-2} M. We want to point out here that the pH values at the different concentrations of the solutions was set by adding increasingly amounts of sulfuric acid (H_2SO_4), which implies that in Figure 4 (right column) an increasing concentration is accompanied with an significant increase of the total ion concentration of the solution. A qualitative, although not yet fully quantitative explanation for this quite unexpected behavior is that the desorption yield depends on the ionic strength of the solution. Increasing ionic strength of the solution will increase the amount of recombining ions and reducing the yield of isolated ions that cannot recombine and which are finally detected in the experiment. Therefore, it appears plausible to assume that the abundance of protonated monomers and dimers in solution is much larger at pH = 2 as opposed to pH = 5, but at the same time both are much less well desorbed due to the smaller escape probability in the overall recombination in the dense laser excited medium.

The non-trivial pH and concentration dependence of the gas phase mass peaks provide evidence for our conclusion that laser induced liquid beam desorption of preformed ions in solution actually images the situation in solution, *i.e.*, it likely projects equilibrium concentrations or populations of preformed non-covalently bound complexes and aggregates in solution into the gas phase. It is foreseeable that this powerful feature can be used to study biopolymers, their aggregates and conformations as well as reactions in solution.

Molecular recognition is a specific non-covalent attraction that takes place at the molecular level. It may be achieved through a variety of interactions: ionic, hydrogen bonding, hydrophobic associations, among others. Most commonly molecular recognition is achieved through a favorable combination of various interactions in solution. In recent experiments, we have employed liquid beam desorption mass spectrometry to desorb mixtures of amino acids in water solutions in order to study the most simplest cases of molecular recognition for relatively small molecular systems. We study these model systems because they are simple enough to understand the interactions on a molecular level. We consider an aggregation specific – that may resemble a molecular recognition – if it is specific for the pair of amino acids under consideration and if they deviate from the normal statistical distribution of dimers and mixed dimers which follows a binomial distribution. In Figure 5 mass spectra of L-ornithine and L-citrulline (10^{-2} mol/l) are displayed for two ion optics gate times (upper two panels of Fig. 5) which are optimized for the protonated monomer and the protonated dimer, respectively. As can be seen, the protonated monomers have comparable intensity. While the relative intensities of the protonated *homo*-dimers are not too different from the relative intensities of the monomers, the abundance of the protonated *hetero*-dimer is significantly larger than the expected statistical ratio of 2:1 for a mixed dimer. We believe that the preferred aggregation of L-ornithine and L-citrulline can be rationalized in terms of the number of specific H-bonds that can be established in the dimers. As discussed above, the ability to show strong dimerization stems from the formation of two salt bridge bonds

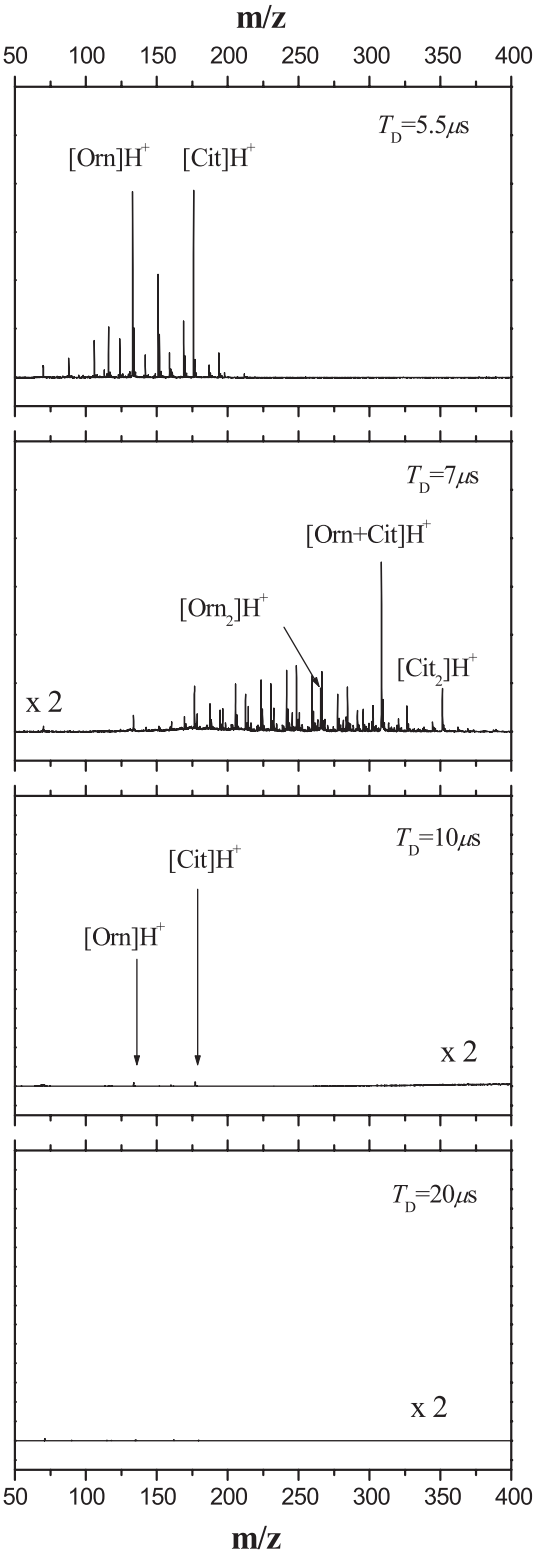

Fig. 5. Desorption of protonated L-ornithine and L-citrulline and their non-covalently bound (mixed) dimers as well as various water clusters from a 10^{-2} M water solution (upper two panels). Shown are traces for ion optics delays, T_D, which are optimized for monomers and dimers, respectively, as well as for later times in the search for possible delayed desorption (lower two panels). Note, at longer times no monomer nor dimer can be detected excluding delayed desorption.

between the carboxylic group and the α-amino group. Based upon chemical intuition we attribute the large abundance of mixed aggregates to their enhanced stability, which is likely a direct consequence of an additional interaction (stabilization) of the protonated terminal amino group of ornithine with the terminal group (R–NH–(CO)–NH_2) in the side chain of citrulline.

To ensure that these amino acid clusters were indeed atypical several other amino acids were run under the same conditions. In particular, arginine, lysine, and histidine were examined due to their high basicity. Under conditions where ornithine and citrulline form large abundances of mixed protonated clusters the others did not show this type of behavior.

Arginine self-assembles large non-covalent singly protonated multimers when sampled by IR laser induced water beam desorption mass spectrometry. The desorption of large protonated arginine aggregates from 0.1 molar aqueous solution is displayed in Figure 6. The progression of aggregates can easily be followed up to the octamer. The propensity for arginine to cluster more than other amino acids is consistent with observations form other groups employing different techniques [16]. While the existence of large protonated arginine assemblies can easily be proven experimentally in this and other experiments, information about their structure is much more difficult to obtain. It has been argued that molecular clusters provide an interesting bridge between the gas- and solid-phase properties of molecules. Given sufficient size, the molecular clusters may begin to exhibit solid-phase characteristics, such as the stabilization of zwitterionic salt bridges through self-solvation [15]. Arginine is the most basic amino acid. This high basicity increases the stability of zwitterionic arginine in the gas phase relative to other amino acids. However, recent experiments have shown that isolated arginine is not a zwitterion [26]. Interestingly, the stability of the zwitterionic forms of amino acids can be substantially modified by specific noncovalent interactions with nearby molecules and ions [15,27]. Recent experiments and theory suggest that the protonated arginine dimer exists with one arginine in the zwitterionic state [15]. The larger the number of arginines present, the easier it becomes to self-solvate charged groups. The extreme example of this is found in crystal structures, where even glycine is stabilized in the zwitterionic state [15,16]. This suggests that it should be possible to stabilize all of the amino acids as zwitterions through self-solvation, provided a sufficient cluster size is attained. For arginine the critical cluster size has been found to be the dimer. Crystalline arginine itself is different from other amino acids. Typically, amino acids arrange themselves in a peptide-like fashion with the N-terminal amino and C-terminal carboxylate groups aligned with the side chains protruding outward on alternating sides [28]. In contrast, arginine stacks end to end (head-to-tail) enabling the guanidinium and carboxylate interactions [29]. This motif is common in crystal structures containing arginine.

The very pronounced non-chiral self recognition of arginine measured in this work is attributed to the highly

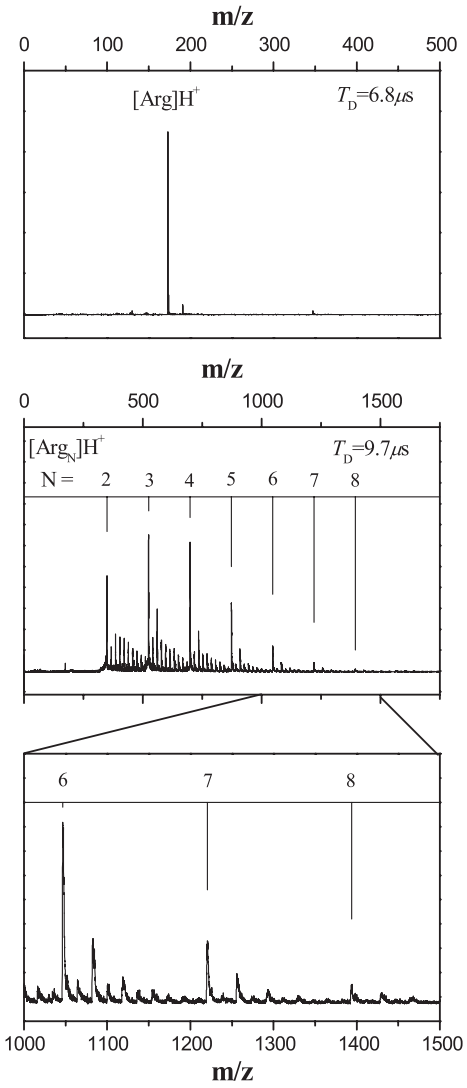

Fig. 6. Large protonated aggregates of arginine (and water) obtained from the IR laser desorption of 10^{-1} M solution of arginine hydrochloride in water. Note, the progression of multimers can be easily followed up to the octamer. Note, the propensity for the protonated arginine water aggregate with $n_{\text{water}} = 2$.

favorable and specific guanidinium/carboxylate interaction. This double salt bridge is additionally stabilized by two strong, specific hydrogen bonds. It has been discussed whether the structures of large protonated clusters like the octamer may actually resemble the crystal structure of arginine (head-to-tail orientation). The question whether such detected aggregates are already preformed in solution and represent early stages of nucleation is currently discussed [30,31].

None of the protonated arginine clusters in this work are unusually abundant in the cluster distribution, suggesting no special stability of the protonated multimers. However, we point out that among the protonated and solvated multimers of $Arg_nH^+(H_2O)_m$ water clusters those with $m = 2$ are unusually abundant. In addition, we have already pointed out the enhanced stability for $((HArg)_2Cl)^+$ aggregates discussed above.

3.2 Desorption mechanism

A general quantitative model for the IR-laser induced desorption of ions – as well as for the MALDI or ESI process – does not exist yet. However, in the case of a laser desorption from a liquid (water) beam the situation is not hopeless because the initial liquid matrix is well defined [20] and its parameters like temperature, viscosity and pH value can be controlled precisely. In principle, two desorption mechanisms can be considered. Kondow *et al.* discuss the limiting case of low desorption laser power [11]. In this case the IR laser pulse only heats up the liquid beam to some extent. The molecules in this case are desorbed from the liquid beam surface. The results of our measurement of the velocity and cluster distribution of desorbed neutral resorcinol (employing excitation at 2 500 nm, a laser power significantly below 10^7 W/cm^2, and post-desorption ionization at 193 nm [32]) was very similar to those obtained by Kondow *et al.* [11] which may indicate that two mechanisms (phases) exist for the desorption, which are accompanied by very different solvent aggregation.

If the absorbed laser energy coupled into the liquid beam is significantly larger, the situation is very different. In this case the IR laser wavelength is tuned to the blue wing of the IR absorption of liquid water (2.8 μm) to match the penetration depth of the IR laser pulse with the beam diameter (12 μm). This ensures a uniform heating of the irradiated volume of the beam and avoids desorption from the surface of the beam due to a small penetration depth. During the laser excitation of a small volume of the liquid jet it can be assumed that the solvent (H_2O) does not evaporate instantaneously but heats up significantly above its critical point. A temperature rise of approximately 350 K can be estimated from the laser power in the focus, the beam waist diameter, the water beam dimensions, the absorption coefficient, and the heat capacity of water. The threshold energy for this process was determined to be around 10^8 W/cm^2. In the supercritical phase some features of the solvent (like the ability to solve ions) are conserved [33]. After the laser induced temperature jump an explosive expansion of the laser excited volume follows, which accelerates solvent as well as solute molecules. During this expansion the density and the dielectricity constant of the solvent decreases. Because of the reduced shielding of the ions due to the solvent, cations and anions recombine to a large extent. Very likely only a small fraction of the total ion concentration in solution (10^{-4}–10^{-8}) can be detected in the gas phase by mass spectrometry. In the present experiment (without a UV ionization laser) we are able to investigate this process employing an ion optics consisting of an acceleration region of 12 mm and a field free drift distance of 35 mm and by gating the second ion optics of the TOF with respect to the desorption laser pulse. Details of the time dependent desorption mechanism are projected onto the drift times of the aggregates. While the first electrode pair (25 mm

spacing) accelerates the ions in a cw-field of 25–100 V/cm and separates different species with different m/z to some extent in the field free drift region (35 mm), the second ion optics is pulsed and accelerates slices out of the distribution of ions. We want to emphasize here that in our case we are sure that we have a one step desorption under our conditions rather than a more complicated time dependence such as reported in reference [11]. This can be inspected in Figure 5 where protonated monomers and dimers from the initial evaporative desorption process arrive in the ion gate at 5.5 μs and at 7 μs, respectively (upper two panels). While at 10 μs at most 1% of the monomer intensity measured at 5.5 μs is observable (possibly from fragmentation) we do not observe any delayed protonated monomer at 20 μs delay. This situation is very different from that described in reference [11]. The question is now: can we learn something about the initial explosive desorption from a supercritical volume that expands rapidly? In order to shed some light into this phenomenon we measured drift times of protonated monomers and multimers and compare it with drift times calculated for isolated molecules. Before, we have checked that drift times of ionized molecules in the gas phase (like benzene cations from a REMPI experiment) exactly follow our predictions. Figure 7 shows ion signals for protonated monomers and multimers. Since the delay times T_D have been adjusted for maximum signal for each species, they are in fact a measure of the flight time in the drift region after desorption and acceleration in a cw field of 100 V/cm. These experimental flight times T_D (•) are compared with calculated flight times (—) for protonated monomers ($N = 1$) and multimers ($N = 2-4$) of lysine in Figure 8. We want to emphasize, that in the calculation of the flight time in the ion optics and in the drift region an acceleration of the cationic species MH^+ to $v_0 \approx 1\,000$ m/s in the initial expansion, and a subsequent acceleration in the ion optics to $v_0 + v_{\text{field}}$ is assumed. Note, v_0 is a parameter in our calculation. A rough initial estimate of the expansion velocity was 1 000 m/s. As can be inspected in Figure 8 the measured delay times are nearly exactly on top of the predicted ones (no time lag) if one assumes actually $v_0 = 1\,000$ m/s. We have found that this parameter may vary for different experimental conditions (*e.g.*, laser energies) within a factor of two. Nevertheless, due to the possibility of a precise experimental determination of drift times for different masses and voltages, v_0 can be determined with high precision in this type of experiment. The measured flight times T_D are determined by an initial explosive expansion phase in which ions can only be accelerated by the dense medium but not by the electric field, and a phase in which the ions are nearly free and accelerated in the ion optics. If we assume a liquid density of the solvent at $t = 0$, a supercritical volume close to the liquid beam dimension after the excitation which is followed by a rapid expansion, it takes roughly about 1 μs to expand the volume to a sphere with a radius of about 1 mm. The effective pressure in the expanded gas is now in the torr range and only at this reduced gas density charged aggregates can be accelerated by the field out of the expansion center. Shortly after this point the mean free

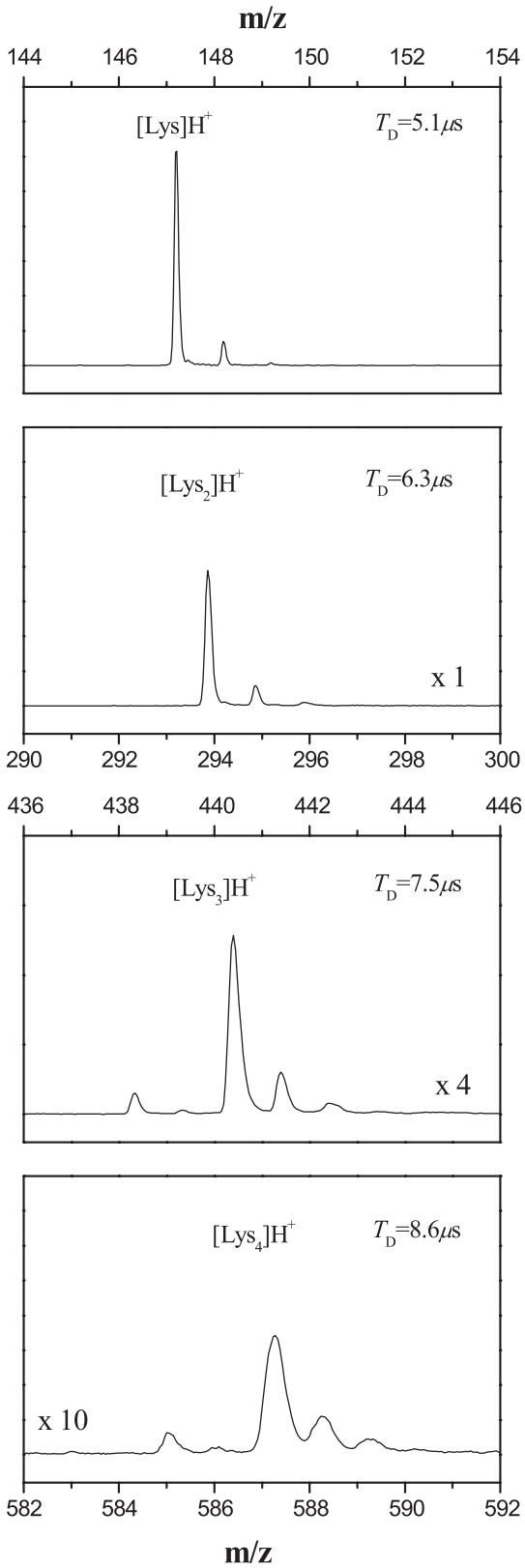

Fig. 7. Drift times T_D (optimized delay times of the ion optics with respect to the desorption laser pulse) for protonated monomers and multimers. Shown are relative intensities. The intensities in panels 3-4 are amplified by a factor of 4 and 10, respectively. For more details see the text.

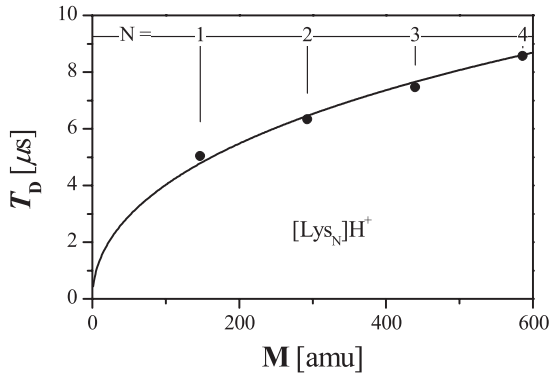

Fig. 8. Calculated (—) and measured (•) flight times T_D for protonated monomers ($N = 1$) and multimers ($N = 2-4$) of lysine. In the calculation of the flight time in the drift region an acceleration of the cationic species MH^+ to $v_0 = 1\,000$ m/s and a subsequent acceleration in the ion optics to $v_0 + v_{\text{field}}$ is assumed. Note, v_0 is a parameter in our calculation.

path length of the solvent and the desorbed molecules are already larger than the dimensions of the vacuum chamber. Therefore, we anticipate interactions only be possible within the first one or two μs of the expansion. In separate experiments we have found that after the expansion the biomolecules have nearly the same speed than the driving gas (H_2O), which increases the kinetic energy of the desorbed molecules significantly [19,32]. This effect is most pronounced and easily observable for large molecular masses and small accelerating voltages (20 V/cm) in the first ion optics.

Although, we have determined some characteristic features of the desorption process, some questions stay open. In particular, it is not completely clear at present if and how the supercritical situation influences or determines the experimental findings. It is evident, however, from the data in the present article that the desorption process is very soft without significant fragmentation (fission of covalent bonds). Even more striking is the observation that the supercritical state apparently does not destroy most of the relatively weakly bound adducts and non covalent bonds in solution. The simplest picture of the process may be a fast laser excitation and subsequent heating of the liquid matrix molecules above the supercritical point without the time for significant thermal equilibration of solute and water molecules which is followed by a subsequent (adiabatic) seeded expansion of the gas. The development of a more detailed dynamic model of the process is in progress at present and will be published in a forthcoming article.

4 Summary and conclusions

In summary, we have demonstrated that analytical laser induced liquid beam desorption mass spectrometry is a versatile and powerful tool for the investigation of protonated amino acids and their non-covalently bound complexes. Our mechanistic studies reveal that biomolecule desorption is a one step process involving laser heating of the solvent above its supercritical temperature followed by a rapid expansion, a nearly quantitative ion recombination, and a subsequent isolation of only a small fraction of preformed ions and charged aggregates. Studies of the pH and concentration dependence of the ion production in the gas phase suggests that – in the case of positively charged ions – the process depends upon the concentration of all ions in solution, the proton affinity of the solvent and the solute, and the pH *of the solution*. An interesting and most important feature of the present technique is that it appears to provide a "snapshot" of the situation in solution (equilibrium concentrations of ionic species, dimerization, conformation, etc.). This feature and the dependence of the desorption probability upon the pH as well as the proton affinity [24] of the molecules in solution may be used as an analytical tool to discriminate biomolecules appearing at similar masses, *e.g.*, in complex mixtures of biomolecules in solution. It adds an additional dimension to the interpretation of complex mass spectra [34]. We have found that arginine easily forms large non-covalent singly protonated multimers in our experiment with structures that may resemble those of the solid state and which may be preformed in solution prior to desorption. Since the desorption is very soft and gentle non-covalently bound complexes, *i.e.*, dimers and mixed dimers could be investigated. The preference for mixed dimers of citrulline and ornithine can be regarded as one of the simplest cases of molecular recognition. We anticipate that the ability to easily monitor non-covalently bound complexes desorbed from water solutions may provide a powerful tool for a rapid screening of target specificity of drugs in the future. If the continuous desorption source is replaced by a droplet source the sensitivity and material consumption is competitive to other analytical techniques like ESI-MS or MALDI-MS.

The authors thank the *Deutsche Forschungsgemeinschaft* (GK782, "Spectroscopy and dynamics of molecular aggregates, coils, chains and networks") and the *Fonds der Chemischen Industrie* for financial support. We also acknowledge discussions of some aspects of the present work with Professor B. Brutschy.

References

1. T. Veenstra, Biophys. Chem. **79**, 63 (1999)
2. J.B. Fenn, M. Mann, C.K. Meng, S.F. Wong, C.M. Whitehouse, Science **246**, 64 (1989)
3. M. Karas, F. Hillenkamp, Anal. Chem. **60**, 2299 (1988)
4. W. Kleinekofort, A. Pfenninger, T. Plomer, C. Griesinger, B. Brutschy, Int. J. Mass Spectrom. Ion Proc. **156**, 195 (1996)
5. W. Kleinekofort, J. Avdiev, B. Brutschy, Int. J. Mass Spectrom. Ion Proc. **152**, 135 (1996)
6. F. Sobott, A. Wattenberg, H.-D. Barth, B. Brutschy, Int. J. Mass Spec. **185-187**, 271 (1999)
7. A. Wattenberg, H.-D. Barth, B. Brutschy, J. Mass Spectrom. **32**, 1350 (1997)
8. A. Wattenberg, F. Sobott, H.-D. Barth, B. Brutschy, Int. J. Mass Spectrom. **203**, 49 (2000)

9. T. Kondow, F. Mafune, Ann. Rev. Phys. Chem. **51**, 731 (2000)
10. J. Kohno, F. Mafune, T. Kondow, J. Phys. Chem. A **105**, 8939 (2001)
11. N. Horimoto, J. Kohno, F. Mafune, T. Kondow, J. Phys. Chem. A **105**, 9569 (1999)
12. E. Bobertson, J.P. Simons, Phys. Chem. Chem. Phys. **3**, 1 (2001)
13. E. Strittmatter, E.R. Williams, J. Phys. Chem. A **104**, 6069 (2000)
14. D.X. Zhang, L.M. Wu, K.J. Koch, R.G. Cooks, Eur. Mass. Spectrom. **5**, 353 (1999)
15. R.R. Julian, J.L. Beauchamp, W.A. Goddard, J. Phys. Chem. A **106**, 32 (2002)
16. R.R. Julian, R. Hodyss, J.L. Beauchamp, J. Am. Chem. Soc. **123**, 3577 (2001)
17. R.A. Jockusch, P.D. William, E.R. Williams, J. Am. Chem. Soc. **119**, 11988 (1997)
18. R.A. Jockusch, W.D. Price, E.R. Williams, J. Phys. Chem. A **103**, 9266 (1999).
19. A. Charvat, E. Lugovoj, M. Faubel, B. Abel, Rev. Sci. Instr. (in press, 2002)
20. M. Faubel, B. Steiner, Ber. Bunsenges. Phys. Chem. **96**, 1167 (1992)
21. M. Faubel, T. Kisters, Nature **339**, 527 (1989)
22. M. Faubel, S. Schlemmer, J.P. Toennies, Z. Phys. D **10**, 269 (1988)
23. B. Brutschy, personal communication
24. E.P.L. Hunter, S.G. Lias, J. Phys. Chem. Ref. Data **27**, 413 (1998)
25. R.M. Wightman, D.O. Wipf, Acc. Chem. Res. **23**, 64 (1990)
26. C.J. Chapo, J.B. Paul, R.A. Provencal, K. Roth, R.J. Saykally, J. Am. Chem. Soc. **120**, 12956 (1998)
27. T. Wyttenbach, M. Witt, M.T. Bowers, J. Am. Chem. Soc. **122**, 3458 (2000)
28. C.G. Suresh, M. Vijayan, Int. J. Pept. Prot. Res. **21**, 223 (1983)
29. J. Karle, I.L. Karle, Acta Cristallogr. **17**, 835 (1964)
30. R.G. Cooks, D. Zhang, K.J. Koch, F.C. Gozzo, M.N. Eberlin, Anal. Chem. **73**, 3646 (2001)
31. R. Hodyss, R.R. Julian, J.L. Beauchamp, Chirality **13**, 703 (2001)
32. A. Charvat, E. Lugovoj, M. Faubel, B. Abel, unpublished results
33. E.U. Franck, R. Deul, Faraday Discuss. **66**, 191 (1978)
34. A. Charvat, E. Lugovoj, M. Faubel, B. Abel, Anal. Chem. (in press, 2002)